Reactive Melt Blending of Modified Polyamide and Polypropylene: Assessment of Compatibilization by Fractionated Crystallization and Blend Morphology

Gisela Pompe, Petra Pötschke, Jürgen Pionteck

Institut für Polymerforschung Dresden e.V, Hohe Straβe 6, D-01069 Dresden, Germany

Received 11 May 2001; accepted 19 April 2002

ABSTRACT: The melting and crystallization behavior of nonreactive and reactive melt-mixed blends of polypropylene and carboxylic-modified polyamide (mPA) as the dispersed phase was investigated. It was found that the size of the mPA particles decreases and the crystallization behavior of the mPA particles changes in dependence on the mixing time of the blends with oxazoline-modified PP (mPP). This indicates that an *in situ* reaction occurs between the oxazoline groups of mPP and the carboxylic acid groups of mPA, resulting in a compatibilizing effect. In blends with mPP, the crystallization of the dispersed mPA phase splits into two steps. Below a critical particle size, the mPA does not crystallize at temperatures typical for bulk crystallization. These finely dispersed mPA particles crystallize coincidently with the PP phase, and this part increases with increasing mixing time. Analysis of the crystallization heat of both steps in connection with the particle volume distribution permits the estimation of the critical particle size to be ≤ 4 μm. These investigations showed that the effect of fractionated crystallization can be used to follow the morphology development and to evaluate the efficiency of compatibilizing interfacial reactions during processing. © 2002 Wiley Periodicals, Inc. J Appl Polym Sci 86: 3445–3453, 2002

Key words: crystallization; blends; polyamides; poly(propylene) (PP); reactive processing

INTRODUCTION

Blends of the immiscible polypropylene (PP) and polyamide (PA) have been studied extensively.[1–7] Without compatibilization of the immiscible components, a coarse morphology is observed, resulting in poor mechanical properties. The properties can be improved by compatibilization both by the addition of interfacial active block copolymers and by the use of functionalized components which can react with each other during processing, forming interfacial active components *in situ*.[8] Consequently, the interfacial tension between the components decreases, and the coalescence of the dispersed phase will be suppressed.[9] Both effects result in smaller particle sizes and more stable morphology during the following processing. In combination with enhanced interfacial adhesion, these effects lead to improved mechanical properties.

Ikkala et al.[5] and Everaert et al.[10] used different additives to compatibilize immiscible blends. In connection with the decreasing particle size, the authors observed the effect of fractionated crystallization[11,12] in the dispersed phase, also called retarded crystallization by Zhang et al.[13]

In the bulk state of the polymer, melt crystallization starts by heterogeneous nucleation and spreads over the whole available material via "second crystallization" before another type of heterogeneity can become efficient.[11] The crystallization is initiated by heterogeneities A_1, which have the smallest surface energy of the crystallites in the melt. This requires the smallest supercooling, $\Delta T_{c,\mathrm{bulk}} = T_m^0 - T_{c,\mathrm{bulk}}$,[11] for the crystallization process, with T_m^0 as the equilibrium melting temperature and $T_{c,\mathrm{bulk}}$ as the crystallization temperature of the pure polymer. The concentration $M(A_1)$ of the heterogeneities A_1 determines the critical volume $V_{d,\mathrm{cr}} = 1/M(A_1)$ of the dispersed particle, in which only one nucleus exists on average, which means, for particle volumes $< V_{d,\mathrm{cr}}$, no heterogeneities of type A_1 exist and, therefore, crystallization cannot occur at $T_{c,\mathrm{bulk}}$. If other heterogeneities A_i acting as nuclei exist and their concentration is sufficient, then these particles can crystallize at lower temperatures $T_{c,i}$., which means that a higher supercooling $\Delta T_{c,i}$ than in the bulk state is required. If such heterogeneous nucleation does not occur in the particle volume, the homogeneous nucleation with the highest possible supercooling of $\Delta T_{c,\mathrm{hom}} = T_m^0 - T_{c,\mathrm{hom}} = 0.2\ T_m^0$ (ref. 14) starts the crystallization.

A stepwise crystallization of the finely dispersed phase is possible, the so-called fractionated crystalli-

Correspondence to: P. Pötschke (poe@ipfdd.de).

Contract grant sponsor: Deutsche Forschungsgemeinschaft (Collaborative Research Centre 287).

zation. The number of the steps is dependent on the chemical structure and the concentration of the nucleating heterogeneities of the dispersed polymer and on the particle-size distribution. It is interesting that the melting behavior is almost independent of the number and the efficiency of the fractionated crystallization steps.

In this work, the thermal behavior and the morphology were investigated for the blend combination PP/PA = 50/50 wt % (≈55/45 vol %), whereby the PA forms the dispersed phase. The PP was grafted with oxazoline monomers and the PA component was terminated by carboxylic acid with the goal of an *in situ* compatibilization between the blend components.

The questions of interest are whether the effect of fractionated crystallization can be observed as a result of the improved dispersity in this reactive blend system and whether a quantitative correlation between the morphology and thermal properties can be established. It will be shown that fractionated crystallization is a proper tool to characterize the compatibilization efficiency.

EXPERIMENTAL

Materials and blend preparation

The virgin PP used for these investigations was Novolen® 1127 MX (BASF AG, Ludwigshafen, Germany). To obtain the reactive PP, the PP was modified with ricinol oxazoline maleinate (Loxamid VEP 8515, Henkel, Germany) using a twin-screw extruder (ZSK 30, Krupp Werner & Pfleiderer, Germany). The oxazoline content of the mPP (M_w = 142,500 g/mol, ρ = 0.913 g/cm^3) was 1.3 wt %.

As blend partner, PA6 SH3 (Leuna AG, Leuna, Germany) modified with trimellitic anhydride by reactive extrusion was used.[15] The product is a carboxylic acid-terminated PA (mPA; M_w = 30,000 g/mol, ρ = 1.130 g/cm^3).

The blends were prepared in a miniature mixing reactor EK-3-5C (NCS, Japan).

PP/PA blends of the composition of 50/50 wt % (≈55/45 vol %) were produced at 230°C with a rotation speed of 60 rpm. The mixing time was varied (3, 15, and 30 min). The blends were pressed out of the mixer as strands. In these blends, the PA component, mPA, with a 45 vol % forms dispersed particles in the PP or mPP matrix (see Figs. 1 and 8).

The prepared blends of mPA and PP are assigned as nonreactive while the prepared blends of mPA and mPP are assigned as reactive. In the reactive blends, the interfacial reaction between the oxazoline groups of the mPP and the terminal COOH groups of mPA during melt-mixing forms the compatibilizing block copolymers, as is described for a large variety of different polymer pairs.[16]

Methods of characterization

Microscopy

To visualize the particles in the blend strands, cryofractures were prepared perpendicular to the strand direction. The particle size of the mPA was determined by scanning electron microscopy (SEM) using cut surfaces after chemically etching of the PA phase with formic acid at room temperature for 24 h. After drying, the etched surfaces were gold-sputtered and analyzed by a LEO 435 VP scanning electron microscope (Leo Elektronenmikroskopie, Germany) using an acceleration voltage of 10 kV.

The micrographs for the quantitative analysis were acquired at a magnification of 5000 (micrograph size 65 × 45 μm) under comparable conditions (brightness, contrast) and quantified using the image analysis program Optimas Version 5.2 (Optimas Corp., USA). The distribution of the equivalent circle diameter was determined for ≥0.75 μm, using at least 1000 particles. The deconvolution of the measured particle size by solving the so-called tomato salad problem is described in the Results and Discussion section.

Differential scanning calorimetry (DSC)

DSC measurements were conducted with a Perkin–Elmer DSC7 (equipped with Pyris-Software, Version 3.51) at a scan rate of ±20 K/min under a N_2 atmosphere in the temperature range from −60 to +250°C. The temperatures and the transition heat were calibrated with In and Pb standards.

The sample mass used was about 10 mg. The first heating scans show effects of different thermal histories as a consequence of nonidentical conditions during the blend processing. Therefore, for the characterization of the thermal properties, the cooling and the second heating scans were used. It could be shown that the crystallization and melting behavior does not change by repeated heating/cooling steps in the DSC. The heat of fusion and crystallization calculated for PA6 were normalized to the PA6 content. The statistical error of the values was estimated from repeating measurements and is smaller than ±1 K for the temperatures and about 5% for the transition heats. In addition, some investigations were performed with special temperature programs described in the Results and Discussion section.

RESULTS AND DISCUSSION

Influence of PP modification on the blend morphology and the thermal behavior of the blends

The blend morphology of the nonreactive and the reactive blends after a mixing time of 30 min was

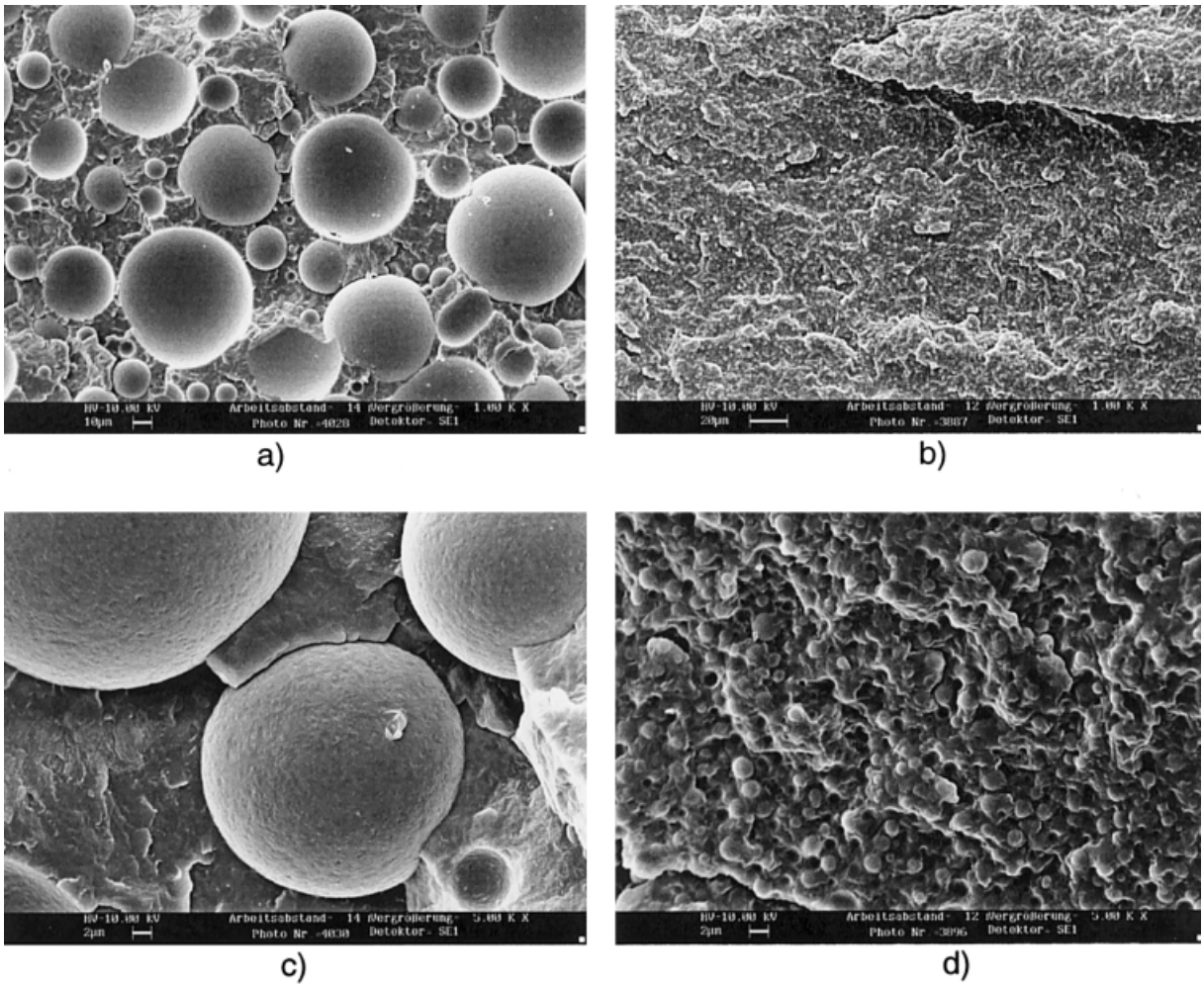

Figure 1 SEM of cryofractures of PP/PA = 50/50 wt % mixed for 30 min, showing the PA6 as dispersed particles: (a,c) nonreactive PP/mPA; (b,d) reactive mPP/mPA [image size 240 × 320 μm for (a,b), 48 × 64 μm for (c,d)].

characterized by cryofractures and is shown in Figure 1. Please notice that the magnification in Figure 1(a,b) is five times lower compared that in Figure 1(c,d). It is obvious that the particle size is much smaller in the reactive blends than in the nonreactive blends, which is attributed mainly to the interfacial reaction, causing an interfacial tension reduction and a significant suppression of coalescence as demonstrated in annealing experiments.[16,17]

The cryofractures also show differences in the phase adhesion. The crack in the nonreactive blend propagates along the interface, and clear surfaces are visible. In the reactive blend, a much better adhesion of the mPA particles to the matrix is visible, which seems to form a thin layer around the particles. In addition, the particles appear more uniform in the reactive blend than in the nonreactive blend.

In Figure 2, the crystallization and melting behavior of both blends after a processing time of 15 min are shown. Additionally, the DSC curves of the pure materials, PP, mPP, and mPA, related to the content in the blend are plotted.

The crystallization and melting behavior in the nonreactive blend correspond to the additive effect of the pure components. No remarkable changes on the degree of crystallinity and the characteristic temperatures were observed. The comparison of the behavior of the crystallization of both pure PPs [Fig. 2(a)] shows that the oxazoline modification has a nucleating effect and so the crystallization temperature of the PP increases.

In the reactive blend, strong changes in the crystallization behavior of the mPA particles are found. The crystallization heat of mPA observed about 190°C is considerably smaller (≈ factor 2) than is the value determined in the nonreactive blend.

However, the melting heat of mPA—as a measure of the mPA crystallinity—is similar in both blends [Fig. 2(b)]. A small exothermic effect appears in the second heating scan of the reactive blend between 180 and 200°C. Apparently, the mPA phase cannot be completely crystallized during the cooling scan. Only when the mobility of the mPP phase is sufficient—as given in the molten mPP state in the second heating

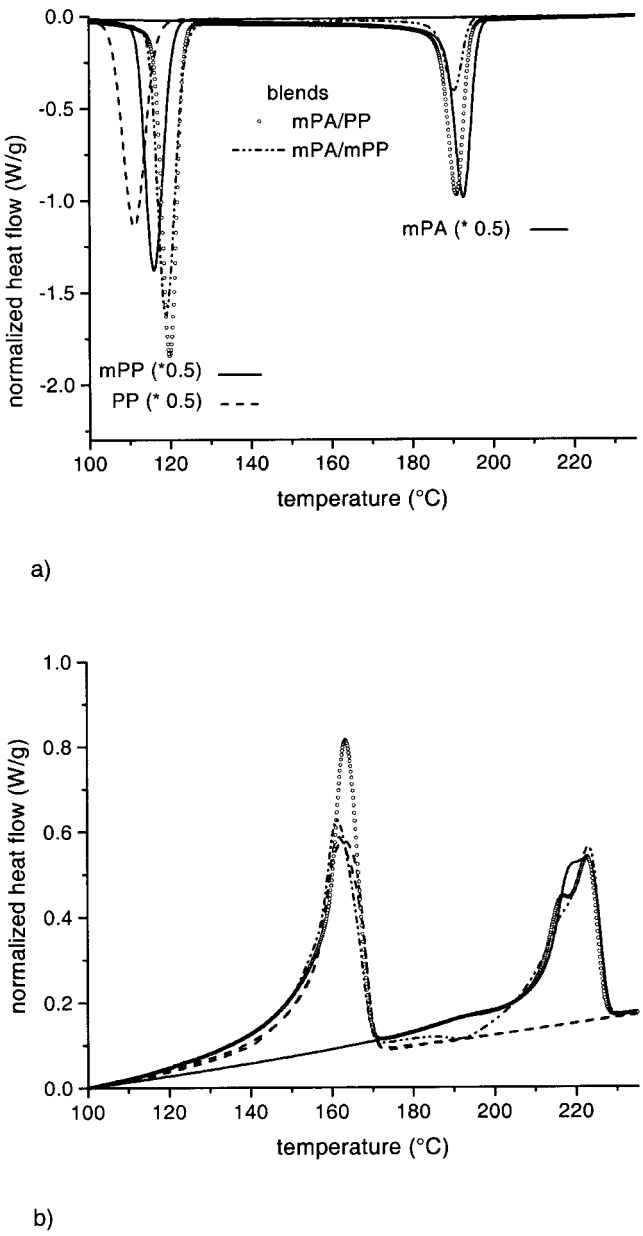

Figure 2 Influence of the PP modification on the thermal behavior of the blends mixed for 15 min: (a) crystallization; (b) melting behavior (2nd heating).

scan—can the residual mPA crystallize in the so-called cold-crystallization process before the PA melting starts at increasing temperatures.

In summary, the thermal behavior of the dispersed mPA blend component is strongly changed by the modification of PP. The effects confirm the morphological results and indicate that the desired interfacial reaction has taken place connected with a compatibilization of both blend components.

We want to remark that the modified PA was used as a blend component for all investigations described in this article. Further studies have shown that the modification of PA6 is not a prerequisite for the observed behavior. Also, unmodified PA6 contains carboxylic end groups in an amount sufficient for reactive *in situ* compatibilization.

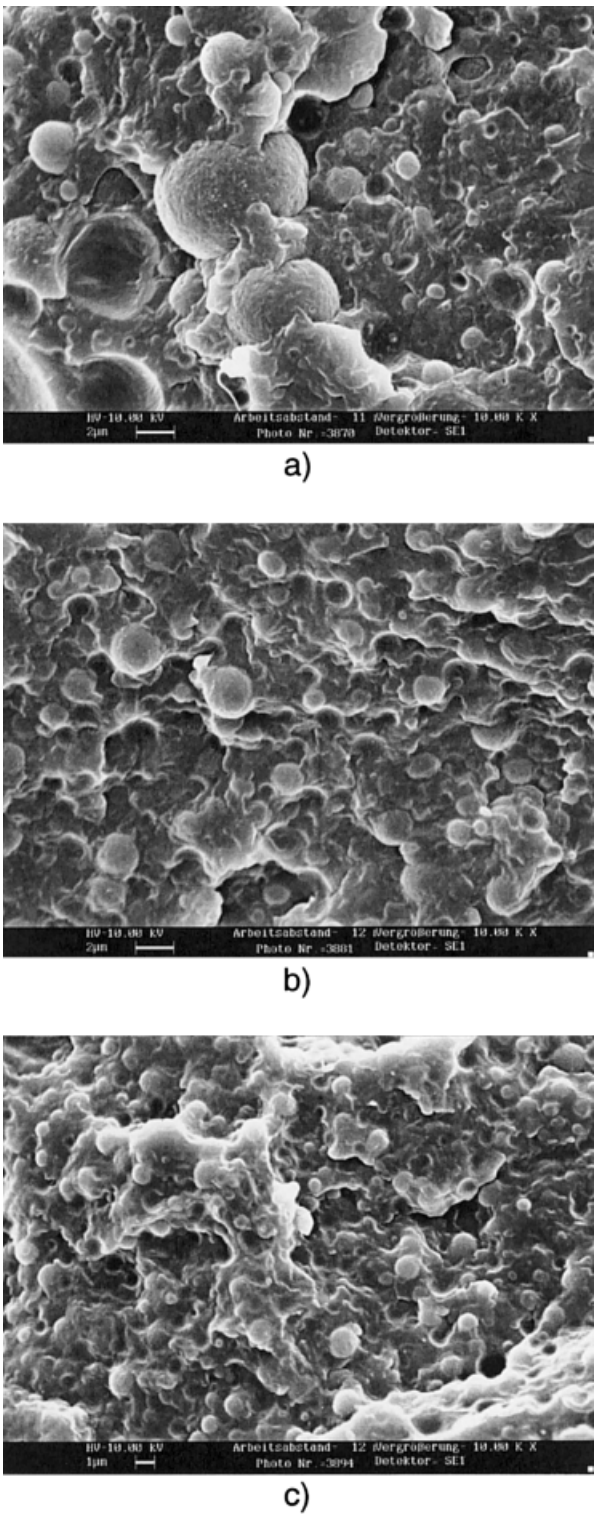

Figure 3 Influence of the mixing time t_p on the morphology in the reactive mPP/mPA blend = 50/50 wt %; SEM of cryofractures; mixing time: (a) 3 min, (b) 15 min, (c) 30 min (image size 24 × 32 μm).

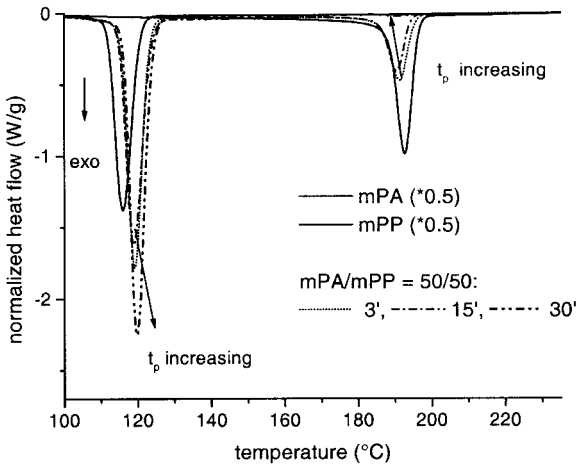

a)

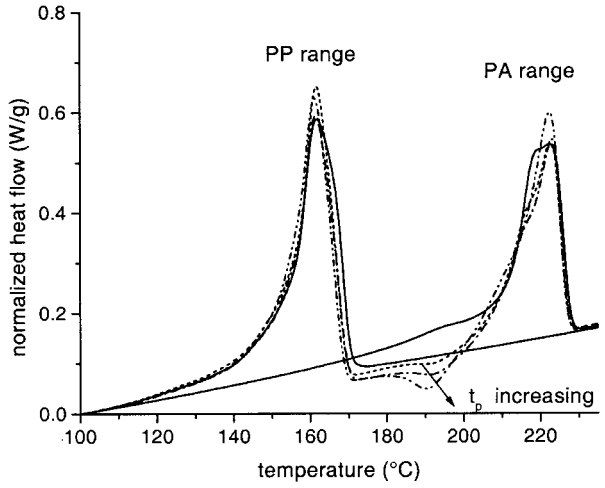

b)

Figure 4 Influence of mixing time t_p on the thermal behavior of the reactive blend of mPP/mPA = 50/50 wt %: (a) crystallization; (b) melting behavior (2nd heating).

Influence of processing time on the blend morphology and the thermal behavior of the reactive blends

The morphology development of the reactive blend mPP/mPA = 50/50 wt % was observed after different mixing times, as shown in the micrographs of cryofractures in Figure 3. The structure after 3 min shows mPP as the matrix with dispersed mPA particles, which are mainly spherical, but have a broad size distribution. The crack propagates along the interfaces, which indicates that an insufficient phase adhesion has been developed. The morphology after 15 min of processing shows smaller spherical mPA6 particles whose size distribution is more narrow. The phase adhesion seems to be enhanced. A thin layer formed by the matrix or *in situ* reaction products surrounds the particles. The longer processing time of 30 min results in a further decrease of the particle size with a more uniform size distribution as compared to the state after 15 min.

Figure 4 shows the corresponding crystallization and melting behavior (2nd heating step). The mPA crystallization is more and more reduced in the temperature range typical for the bulk mPA phase as a consequence of the increasing processing time t_p. After 30 min, the crystallization is almost suppressed in this range. Simultaneously, the crystallization heat in the temperature range of the mPP crystallization increases, as well as the exothermic effect observed in the temperature range from 180 to 205°C in the following heating scan.

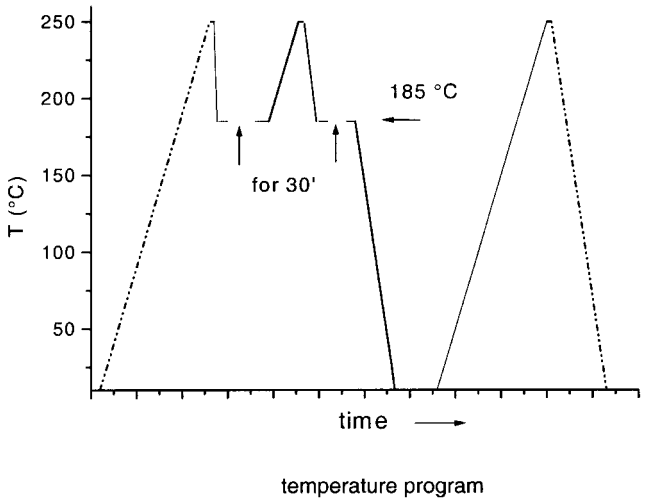

a)

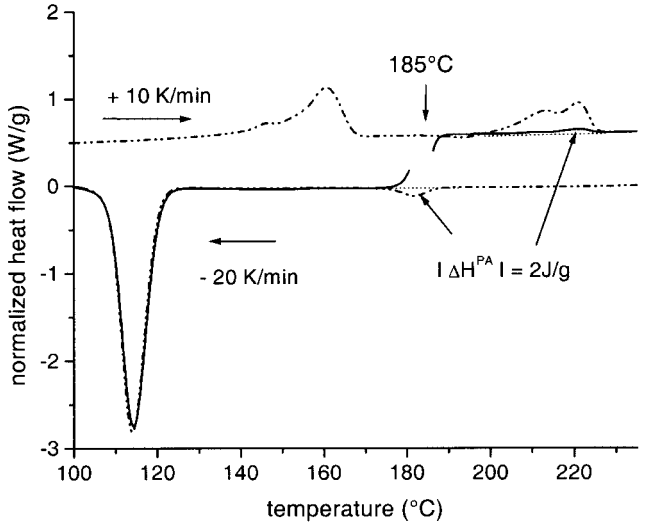

b)

Figure 5 Isothermal crystallization at 185°C of the reactive blend of mPP/mPA = 50/50 wt % mixed for 30 min: (a) temperature program; (b) DSC curves.

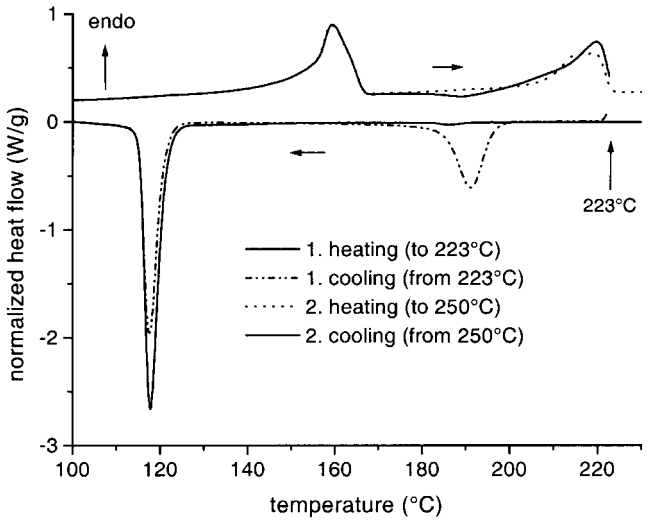

Figure 6 Self-seeding experiment with the reactive blend of mPP/mPA = 50/50 wt % mixed for 30 min (see also text).

The DSC measurements show that the crystalline part of the mPA crystallized at 190°C ($\Delta H_{c,1}/\Delta H_c$) was reduced to 40% after a 15-min processing time and nearly to zero after 30 min. This indicates that the particle size in the blend state after 30 min should already be smaller than the critical particle size.

Further DSC investigation of the reactive blend

Further DSC investigations were carried out on the reactive blend after 30 min mixing time. The crystallization of the dispersed mPA phase in the temperature range typical for the bulk behavior was nearly suppressed in this blend state. Only a small exothermic heat of about −2 J/g with a peak temperature of 185°C was measured.

With the isothermal crystallization at 185°C for 30 min, we tried to check whether the mPA part crystallized about 185°C ($\Delta H_{c,1}$) can be increased by further thermal treatment. The temperature cycle of this experiment and the DSC curves are shown in Figure 5(a). The heating scan started at 185°C after the isothermal treatment [Fig. 5(b)] shows a small melting heat of about 2 J/g. The achieved crystallinity is in the same order as that realized by the dynamical crystallization at the temperature of 185°C. This is a hint that the reduced mPA crystallization at a temperature of about 190°C is not caused by a changed crystallization kinetics.

The self-seeding behavior[18,19] was tested by heating the sample to temperatures (222 and 223°C) between the peak and the end temperature of the mPA melting range (Fig. 6). As expected, the incompletely molten crystallites act as self-seeded nuclei in all mPA particles, independent of their size. Under this condition, the whole crystallization of mPA takes place about 190°C. The heating scan after self-seeding crystallization agrees qualitatively and quantitatively with the bulk behavior of mPA. Before and after the self-seeding process, the sample was completely molten by heating to 250°C. The results confirm the reproducible behavior of the stepwise-fractionated crystallization shown in Figure 4.

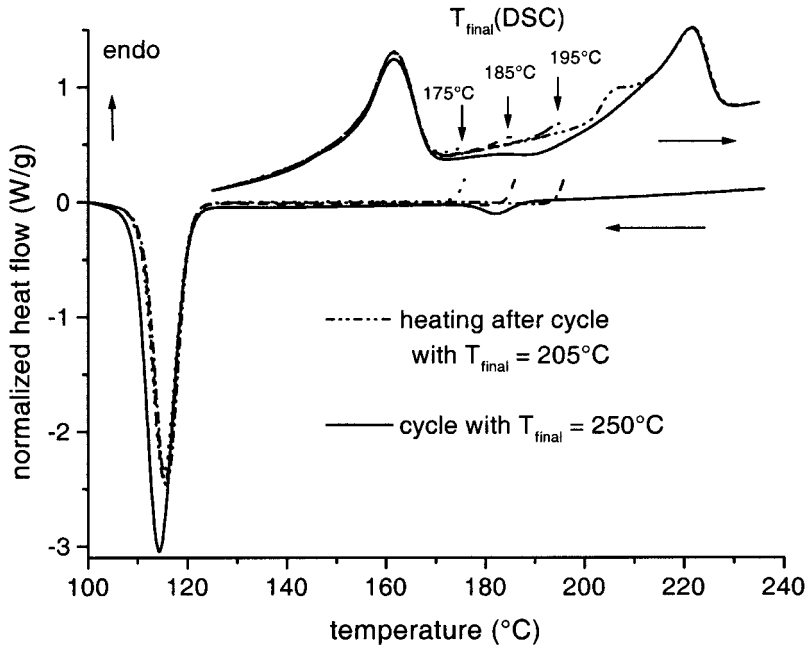

Figure 7 Special thermal DSC regime with increasing final temperature of the heating scans for the reactive blend of mPP/mPA = 50/50 wt % mixed for 30 min.

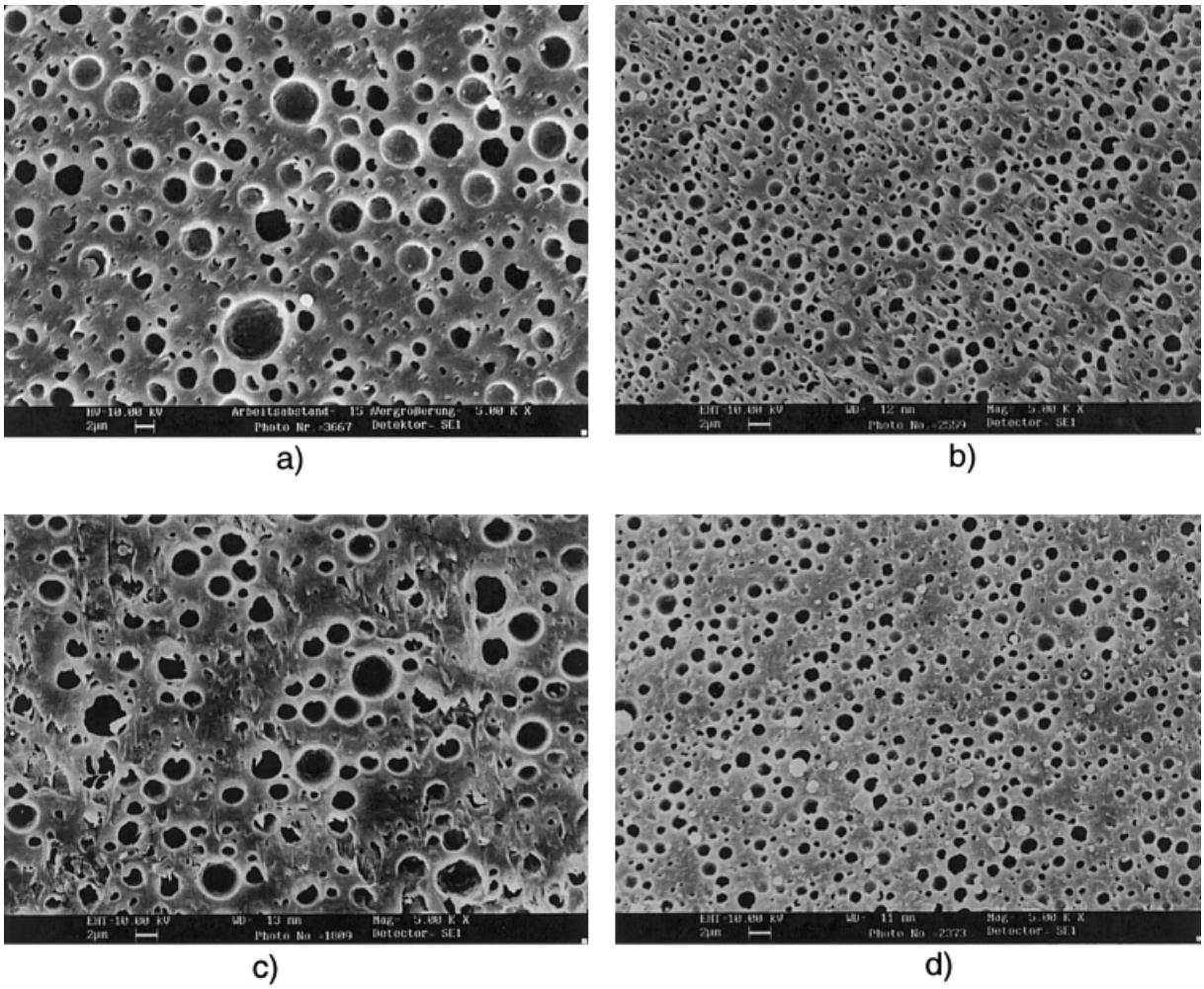

Figure 8 Comparison of blend morphology of mPP/mPA = 50/50 wt % by SEM of etched surfaces (a,b) before and (c,d) after DSC treatment for (a,c) mixed 15 min and (b,d) 30 min (image size 48 × 64 μm).

For the quantitative calculation of all crystallization steps and for the check of the balance, a stepwise heating and cooling program with different final temperatures was carried out (Fig. 7). Two crystallization steps of dispersed mPA exist in the cooling scan: (i) about 180–190°C, typical for bulk behavior ($\Delta H_{c,1}$), and (ii) together with the mPP ($\Delta H_{c,2}$). The third step is the cold-crystallization (ΔH_{cc}) in the following heating scan. The summarized crystallization heats correspond to the melting heat ΔH_f . The crystallization heat of the three steps related to the melting heat (ΔH_f) of mPA gives the values of 7% (for $\Delta H_{c,1}$), 73% (for $\Delta H_{c,2}$), and 20% (for ΔH_{cc}), respectively.

Correlation of morphological data and DSC results

From the results of the morphological and DSC investigations, the critical particle size d_{cr} for the fractionated crystallization of mPA can be estimated. We have shown that the *in situ* interfacial reaction between the modified blend components results in a compatibilization connected with a finer dispersed blend morphology and the appearance of fractionated crystallization. The effect of the fractionated crystallization of the dispersed blend phase can be explained by the existence of a critical particle size d_{cr}.[11] The crystallization in particles smaller than d_{cr} does not take place at temperatures typical for the bulk behavior.

Next, we will consider the results of DSC and morphology investigations to estimate the critical particle size d_{cr} of the mPA. For this, the blend state after the mixing time of 15 min is suitable because mPA crystallizes during the cooling scan both at 190°C ($\Delta H_{c,1}$) and also together with mPP about 120°C ($\Delta H_{c,2}$). The values $\Delta H_{c,1}$ and $\Delta H_{c,2}$ correlate with the crystallization of particles with sizes $d \geq d_{cr}$ and $d < d_{cr}$, respectively. In this way an estimation of d_{cr} should be possible, if the particle-size distribution could be obtained.

First, we proved that the morphology is unchanged after the thermal treatment during the DSC investigations. A comparison between the morphology of the

state before and after the DSC measurements for the blends after the mixing time of 15 and 30 min is given in Figure 8 (etched surfaces of cryocuts). It is obvious that the morphology is almost the same. Therefore, the morphological data obtained for the blend directly after the mixing can be correlated with the DSC results of the cooling scan. From micrographs like the one in Figure 8(a), we obtained the equivalent circle diameter of the particles. Since in morphological analysis based on cuts through a sample the cut plane usually does not go through the center of the spherical particles, the visible circle diameter is smaller than the real one of the particles. This was described by Russ[20] as the "tomato salad problem." The author derived the correction factor of $4/\pi$ for a monodispersed system which was shown also to be applicable for the mean particle diameter in polydispersed systems.[21] The histogram of such a deconvoluted particle diameter is given in Figure 9(a).

The total mPA volume, calculated as the summation of the different particle volumes [$= N(d_n)\ V(d_n)$, see Fig. 9(b)], can be divided into two fractions:

$$V_1 = \Sigma\ N(d_n)\ V(d_n) \text{ with } d_{\max} > d_n \geq d_{cr} \quad (1a)$$

and

$$V_2 = \Sigma\ N(d_n)\ V(d_n) \text{ with } 0 < d_n < d_{cr} \quad (1b)$$

$N(d_n)$ is the number, and $V(d_n)$, the volume of particles of the diameter d_n. We assume that the crystallization heats $\Delta H_{c,1}$ and $\Delta H_{c,2}$ are the result of the crystallization of the two mPA volume fractions V_1 and V_2, respectively.

Under the conditions that—on average—the specific crystallization heat, the density of the crystalline mPA, and the crystallinity are nearly the same in both crystallization steps, the relations follow:

$$V_1/V = \Delta H_{c,1}/\Delta H_c = 0.4 \text{ and}$$
$$V_2/V = \Delta H_{c,2}/\Delta H_c = 0.6 \quad (2)$$

$$V_1/V_2 = \Delta H_{c,1}/\Delta H_{c,2} \approx 0.67 \quad (3)$$

The value of the critical particle size d_{cr} can be estimated using eqs. (1a) and 1(b) and the condition $V_1 \approx 0.67\ V_2$ [see eq. (3)]. From this, we got $d_{cr} \leq 3.8\ \mu m$. Considering all the assumptions leading to the estimation, a range of $3.5\ \mu m < d_{cr} \leq 4\ \mu m$ seems to be reasonable. With the histogram, we establish that only about 6% of all mPA particles have a size with $d \geq d_{cr}$. These particles contribute 40% to the whole crystallization heat during the cooling scan.

The value of d_{cr} describes the concentration $M(A_1)$ of the heterogeneous nuclei A_1 which initiated the mPA crystallization at the smallest supercooling (at 190°C).

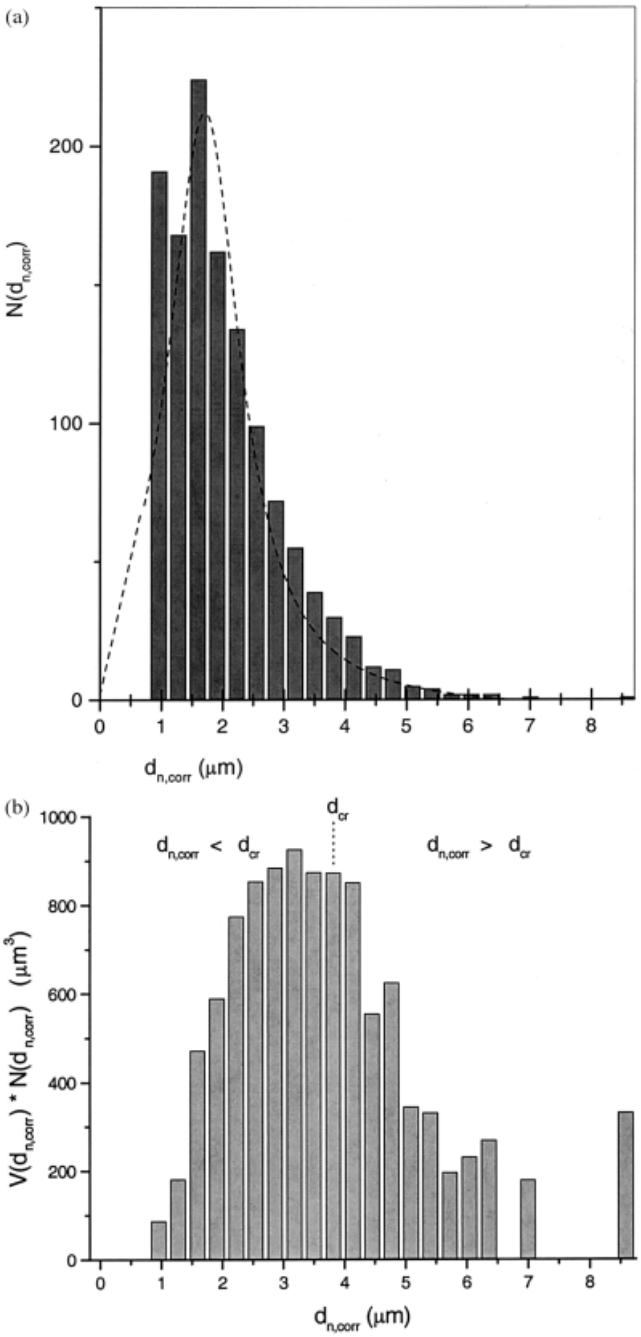

Figure 9 (a) Number N of mPA6 particles in dependence on the deconvoluted circle diameter $d_{n,corr}$ in the reactive blend of mPP/mPA = 50/50 wt.% mixed for 15 min; (b) mPA particle volume [$N(d) \times V(d)$] in dependence on the deconvoluted circle diameter $d_{n,corr}$ in the reactive blend mPP/mPA = 50/50 wt % mixed for 15 min.

Thus, we get for $M(A_1)$ in the mPA used about 10^{10} cm^{-3}.

CONCLUSIONS

We investigated the melting and crystallization behavior of nonreactive and reactive blends based on PP as

the matrix component and PA as the dispersed phase. In the reactive blends, the oxazoline-grafted PP reacted apparently with the carboxylic acid end groups of the PA. This reaction results in a compatibilization connected with a significant particle-size reduction. The compatibilized blends show fractionated crystallization which depends on the degree of dispersity of the mPA phase. The mPA6 crystallization is strongly reduced at temperatures near 190°C, typical for the bulk behavior of PA6. Simultaneously, the transition heat in the range of the mPP crystallization increases. Otherwise, the melting behavior of the mPA crystallites is not strongly affected by the different behavior of the mPA6 crystallization.

Some tests were carried out for a better understanding of the problem using the reactive blend state after a mixing time of 30 min. In this blend state, the crystallization at 190°C is nearly completely suppressed. It was shown that the small residual part of mPA6 crystallized in the 190°C range cannot be enhanced by isothermal crystallization at 185°C for 30 min. However, self-seeded nuclei in the form of incompletely molten mPA crystallites result in a mPA crystallization process similar to the behavior in the bulk mPA.

Eventually, we correlated the DSC results with the morphological data. In the blend state in which mPA crystallized both at 190°C and together with the mPP phase, the critical particle diameter of the mPA particles was estimated. mPA particles with this critical particle diameter contain only one of the heterogeneous nuclei. These nuclei start the crystallization in the bulk state. For the mPA used in this study, the critical particle size was estimated to be in the range of 3.5–4 μm.

Our investigations showed that the fractionated crystallization can be used as a measure for the morphology development. That means that DSC analysis of the crystallization behavior in this blend system is a suitable way for the assessment of the efficiency of the *in situ* compatibilization process.

The authors are grateful for the support of this work by the Deutsche Forschungsgemeinschaft (Collaborative Research Centre 287). The authors thank Andreas Opfermann and Dr. Dieter Lehmann for providing the blends and modified PA6, respectively.

References

1. Beltrame, P. L.; Castelli, A.; Canauz, M. Macromol Chem Phys 1995, 196, 2751.
2. Tang, T.; Huang, B. J Appl Polym Sci 1994, 53, 355.
3. Campoy, I.; Arribas, J. M.; Zaporta, M. A. M.; Marco, C.; Gomez, M. A.; Fatou, J. G. Eur Polym J 1995, 31, 475.
4. Moon, H.-S.; Ryoo, B.-K.; Park, J.-K. J Polym Sci Polym Phys 1994, 32, 1427.
5. Ikkala, O. T.; Holsti-Miettinen, R. M.; Seppälä, J. J Appl Polym Sci 1993, 49, 1165.
6. Franzheim, O.; Rische, T.; Stephan, M.; MacKnight, W. J. Polym Eng Sci 2000, 40, 1143.
7. Parski, M.; Pracella, M.; Galeski, A. Polymer 2000, 41, 4923.
8. Ajji, A.; Utracki, L. A. Polym Eng Sci 1996, 36, 1574.
9. Favis B. D. In Polymer Blends; Paul, D. R.; Bucknall, C. B., Eds.; Wiley: New York, 2000; Vol. 1, Chapter 16.
10. Everaert, V.; Groeninckx, G.; Aerts, L. Polymer 2000, 41, 1409.
11. Frensch, H.; Harnischfeger, P.; Jungnickel, B.-J. In Multiphase Polymers: Blends and Ionomers; Utracki, L. A.; Weiss, R. A., Eds.; ACS Symposia Series; American Chemical Society: Washington, DC, 1989; Chapter 5.
12. Frensch, H.; Jungnickel, B.-J. Colloid Polym Sci 1989, 267, 16.
13. Zhang, X.; Li, G.; Li, J.; Yin, J. Angew Makromol Chem 1997, 248, 189.
14. Turnbull, D.; Cech, R. E. J Appl Phys 1950, 21, 804.
15. Eichhorn, K.-J.; Lehmann, D.; Voigt, D. J Appl Polym Sci 1996, 62, 2053.
16. Liu, N. C.; Baker, W. E. In Reactive Modifiers for Polymers; Al-Maleika, S., Ed.; Chapman and Hall: London, 1997; Chapter 4.
17. Datta, S.; Lohse, D. J. Polymeric Compatibilizers—Uses and Benefits in Polymer Blends; Carl Hanser: Munich, Vienna, New York, 1996.
18. Frensch, H.; Jungnickel, B.-J. Plast Rubb Compos Process Appl 1991, 16, 5.
19. Manaure, A. C.; Müller, A. J. Macromol Chem Phys 2000, 201, 958.
20. Russ, J. C. Practical Stereology; Plenum: New York, 1986.
21. Pötschke, P.; Wallheinke, K.; Janke, A.; Bellmann, C.; Stutz, H.; Heckmann, W. J Macromol Sci Phys B 1999, 38, 527.